


**AUTHOR QUERY FORM**

 <b>ELSEVIER</b>	<b>Journal:</b> AEA  <b>Article Number:</b> 12123	<b>Please e-mail or fax your responses and any corrections to:</b>  <b>E-mail:</b> <a href="mailto:corrections.esco@elsevier.tnq.co.in">corrections.esco@elsevier.tnq.co.in</a>  <b>Fax:</b> +31 2048 52789
--	---	---

Dear Author,

Please check your proof carefully and mark all corrections at the appropriate place in the proof (e.g., by using on-screen annotation in the PDF file) or compile them in a separate list. Note: if you opt to annotate the file with software other than Adobe Reader then please also highlight the appropriate place in the PDF file. To ensure fast publication of your paper please return your corrections within 48 hours.

For correction or revision of any artwork, please consult <http://www.elsevier.com/artworkinstructions>.

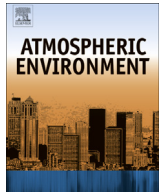
Any queries or remarks that have arisen during the processing of your manuscript are listed below and highlighted by flags in the proof.

<b>Location in article</b>	<b>Query / Remark: Click on the Q link to find the query's location in text Please insert your reply or correction at the corresponding line in the proof</b>
<b>Q1</b>	<p>Please confirm that given names and surnames have been identified correctly.</p> <div data-bbox="304 1102 895 1278"> <p>Please check this box or indicate your approval if you have no corrections to make to the PDF file</p> <input data-bbox="791 1161 879 1242" type="checkbox"/> </div>

Thank you for your assistance.

Contents lists available at [SciVerse ScienceDirect](http://www.sciencedirect.com)

## Atmospheric Environment

journal homepage: [www.elsevier.com/locate/atmosenv](http://www.elsevier.com/locate/atmosenv)Measurements and simulation of speciated PM<sub>2.5</sub> in south-west EuropeQ1 C. Milford<sup>a,b,\*</sup>, N. Castell<sup>c</sup>, C. Marrero<sup>b</sup>, S. Rodríguez<sup>b,a</sup>, A.M. Sánchez de la Campa<sup>a</sup>,  
R. Fernández-Camacho<sup>a</sup>, J. de la Rosa<sup>a</sup>, A.F. Stein<sup>d</sup><sup>a</sup> Centre for Research in Sustainable Chemistry (CIQSO), Joint Research Unit to CSIC "Atmospheric Pollution", University of Huelva, Campus El Carmen, Huelva, Spain<sup>b</sup> Izaña Atmospheric Research Centre, AEMET Joint Research Unit to CSIC "Studies on Atmospheric Pollution", Santa Cruz de Tenerife, Canary Islands, Spain<sup>c</sup> NILU – Norwegian Institute for Air Research, PO Box 100, NO-2027 Kjeller, Norway<sup>d</sup> Earth Resources and Technology on Assignment to Air Resources Laboratory, National Oceanic and Atmospheric Administration, Silver Spring, MD, USA

## HIGHLIGHTS

- A detailed PM<sub>2.5</sub> chemical composition measurement dataset is presented.
- CAMx with high spatial and temporal resolution is evaluated against speciated PM<sub>2.5</sub>.
- Results show important role of non-ammonium nitrate and sulphate in southern Europe.
- Black Carbon is measured and simulated with hourly resolution at two sites.
- Scenarios of pollution events influencing air quality in this region are identified.

## ARTICLE INFO

## Article history:

Received 26 February 2013

Received in revised form

11 April 2013

Accepted 15 April 2013

## Keywords:

PM<sub>2.5</sub> chemical speciation

Air quality

CAMx

Model evaluation

## ABSTRACT

Chemically speciated concentrations of PM<sub>2.5</sub> (sulphate, ammonium, nitrate, elemental and organic carbon) were simulated in south-west Europe using the three-dimensional air quality model CAMx driven by the MM5 meteorological model. The inner domain covered the south-west region of Spain with a high spatial (2 km × 2 km) and temporal resolution (1 h). The simulation results were evaluated against experimental data obtained in four intensive field campaigns performed in 2008 and 2009 at urban and rural sites. PM<sub>2.5</sub> measurements of secondary inorganic compounds and carbonaceous aerosol plus a suite of major and trace elements were determined. High time resolution (10 min) measurements of Black Carbon (BC) were also conducted. The model captured the variability in the ammonium concentrations in both summer and winter periods, although it tended to underestimate the magnitude of concentrations, while for sulphate the performance was better during the summer periods. Particulate ammonium nitrate was only simulated in significant concentrations in the wintertime campaign. This was found to be consistent with the measured composition of PM<sub>2.5</sub> where most of nitrate (79–94%) and a significant fraction of sulphate (24–37%) were estimated to be present as non-ammonium salts. These non-ammonium nitrate salts were attributed to the formation of NaNO<sub>3</sub>. The model PM<sub>2.5</sub> primary elemental carbon simulations, evaluated with hourly resolution, captured the diurnal and seasonal variability of PM<sub>2.5</sub> BC concentrations at the urban site while poorer performance was observed at the rural site. A large underestimation was observed for simulated PM<sub>2.5</sub> organic carbon concentrations during all campaigns. Scenarios of pollution events linked to emissions from south-west Spain, shipping and contributions from more distant emission sources such as Portugal were identified. These results highlight how the distinct features of PM<sub>2.5</sub> composition in southern Europe regions, such as the large contribution of non-ammonium salts, need to be taken into account both in model evaluation and in future implementation of aerosol modelling systems.

© 2013 Elsevier Ltd. All rights reserved.

\* Corresponding author. Centre for Research in Sustainable Chemistry (CIQSO), Joint Research Unit to CSIC "Atmospheric Pollution", University of Huelva, Campus El Carmen, Huelva, Spain.

E-mail address: [cmilford@aemet.es](mailto:cmilford@aemet.es) (C. Milford).

## 1. Introduction

Atmospheric aerosol or particulate matter (PM) is known to have adverse effects on human health (Lopez et al., 2006; Pope and

Dockery, 2006), visibility and both direct and indirect influences on climate (IPCC, 2007). Research over the last decade has indicated that fine particles, generally measured as  $PM_{2.5}$  (particles with aerodynamic diameter  $< 2.5 \mu m$ ) may be more hazardous than larger particles due to the smaller particles penetrating more deeply into the lung and reaching the alveolar region (WHO, 2006; Schlesinger et al., 2006).

The levels and composition of  $PM_{2.5}$  experience variation across Europe. As well as differences in emissions across regions, there also exist meteorological differences, for example in northern Europe the meteorology favours the frequent renovation of air masses while low synoptic wind speeds and low rainfall rates in southern Europe hinder air mass renovation and favour the accumulation of PM (e.g. Rodríguez et al., 2007a). There are also specific component differences, for example the spatial distribution of ammonia emissions and lower temperatures and higher humidity favour formation of ammonium nitrate in northern Europe whereas the formation pathways of  $Ca(NO_3)_2$  and  $NaNO_3$  are significant in Spain from mid-spring to mid-autumn (Rodríguez et al., 2002; Querol et al., 2008).

In addition to European gradients in PM characteristics, significant differences within Spain have been reported (Querol et al., 2008). Secondary inorganic aerosol concentrations at rural and urban background sites in western Andalusia have been found to be higher than those measured in the rest of Spain (de la Rosa et al., 2010). Andalusia is the southern-most autonomous region of Spain and its high concentrations have been attributed to high emissions plus climate factors such as low rainfall and high photochemical activity (Sánchez de la Campa et al., 2007).

Photochemical modelling has developed substantially over the last few decades and is now accepted as a powerful tool to aid and complement air quality studies and assess interactions with climate. A number of aerosol modelling studies in the USA have focused on the eastern or central United States (e.g. Baker and Scheff, 2007; Tesche et al., 2006; Gaydos et al., 2007; Mathur et al., 2008) using large scale measurement networks for their evaluation. There have been various modelling studies in Europe including comparisons with measured speciated aerosol such as Lazaridis et al. (2005), Beekmann et al. (2007), Chemel et al. (2010), Renner and Wolke (2010), Lonati et al. (2010), Andreani-Aksoyoglu

et al. (2011), Schaap et al. (2011), Basart et al. (2012) and Pay et al. (2011). The modelling performance reported depends on component, season and location but the majority of these studies have reported an underestimation of observed concentrations.

One of the limitations in the evaluation of aerosol models is the availability of high quality measurement datasets for evaluation. Routine measurement networks often lack spatial or temporal resolution and are limited to a few aerosol components. This paper presents the evaluation of the photochemical model CAMx against detailed measurements of chemically speciated  $PM_{2.5}$  for a south-west region of Europe. Four intensive measurement campaigns were conducted in September, October 2008 and March and July 2009.  $PM_{2.5}$  composition was obtained at three sites (urban and rural) with 9 h resolution for sulphate, nitrate, ammonium, sea salt, mineral dust and trace elements, and with 1 h resolution of black carbon.

The structure of the paper is as follows. Section 2 describes the study area, model set up, observational data and synoptic meteorology during the campaigns. Section 3 includes results and discussion of the evaluation of the model simulations, plus a brief analysis of regional pollution scenarios while Section 4 provides the conclusions.

## 2. Methodology

### 2.1. Study area

The study area is situated in the western part of Andalusia in Spain and includes the city of Huelva in the west (149,000 inhabitants), Seville (700,000 inhabitants) and the Gibraltar strait in the east (Fig. 1, D03). The topography of the study region has a significant influence on the dispersion and transport of air pollutants (Castell et al., 2010b).

### 2.2. Model description and set up

The photochemical model chosen for this study was the Comprehensive Air-quality Model with eXtensions (CAMx) version 4.51 (ENVIRON, 2008). CAMx is a three-dimensional Eulerian photochemical model including both photo-oxidant

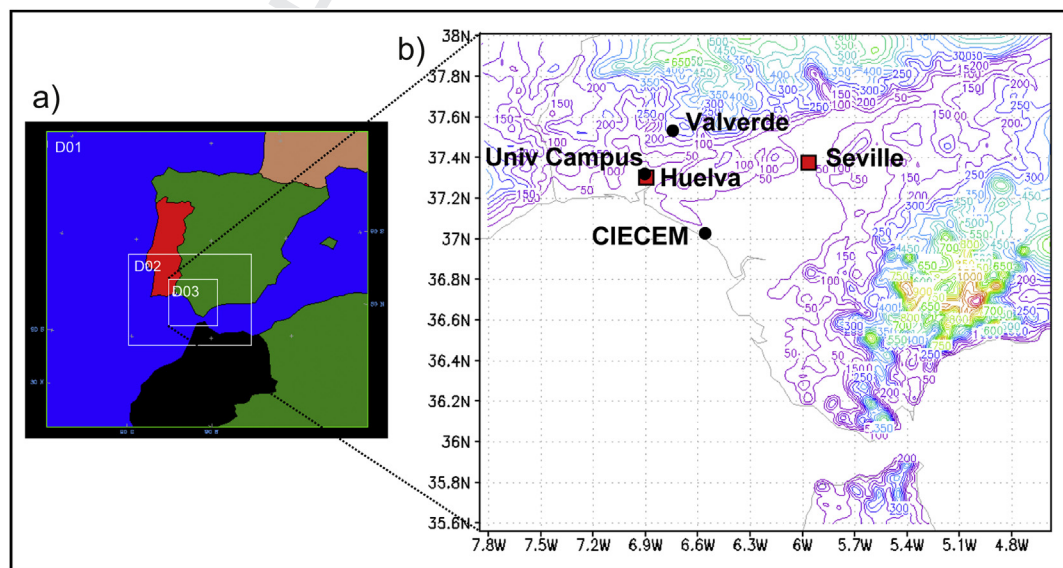


**Fig. 1.** a) Location of the three model domains (D01, D02 and D03) and b) terrain height (m a.s.l.) of the inner domain (D03) with horizontal resolution  $2 km \times 2 km$ . Also indicated are the locations of the measurement sites (Valverde, University Campus and CIECEM) and major cities (Huelva and Seville).

and aerosol chemistry. In this application the CB05 chemical mechanism (Yarwood et al., 2005) and the CF aerosol scheme were implemented.

The model incorporates the ISORROPIA thermodynamic module for partitioning of inorganic aerosols (Nenes et al., 1998, 1999), aqueous-phase chemistry (Chang et al., 1987) and SOAP (Strader et al., 1999) for partitioning of condensable organic gases to secondary organic aerosols. CAMx was run with three nested domains with  $18 \times 18$  km,  $6 \times 6$  km and  $2 \times 2$  km horizontal resolution. The outer domain (D01) covers the Iberian Peninsula, the intermediate resolution domain (D02) includes part of southern Spain and southern Portugal while the inner domain (D03) covers the southwest region of Spain (see Fig. 1). The initial and boundary conditions for the photochemical modelling outer domain were based on Castell et al. (2008). The initial and boundary conditions for ozone (35 ppb) were selected as average background concentrations for the area, while for the other gaseous species clean air conditions were assumed. Initial and boundary conditions for aerosol species were assumed to be zero for this implementation. To minimize the sensitivity of the results to the initial conditions, a spin-up of 72 h was carried out prior to each campaign simulation.

Meteorological input data were provided by the non-hydrostatic Mesoscale Meteorological model (MM5) v3.7 (Grell et al., 1995). Three nested grids (two-way) with the same 18, 6 and 2 km horizontal resolution were used. MM5 was run with 30 vertical layers in a terrain following coordinate system. CAMx was run with 16 of the first 18 vertical layers used in MM5, with increasing vertical resolution closer to the surface. The model top corresponds to approximately 550 hPa while the surface layer corresponds to about 35 m above ground. Initial and boundary conditions for MM5 were obtained from the European Centre for Medium-range Weather Forecasts (ECMWF) numerical weather prediction model analysis at six hourly intervals with a resolution of  $0.25^\circ$ .

### 2.3. Emissions

The emission inventory used in this study was based on Castell et al. (2010a). The outer domains include anthropogenic emissions from the European Monitoring and Evaluation Program (EMEP) emission inventory for the reporting year 2008 (<http://www.emep.int>) and biogenic emissions of non-methane volatile organic compounds (NMVOC) as detailed below. The EMEP 50 km emissions were interpolated to 18 km and 6 km spatial resolution. Emissions in the inner domain include those from industrial activities, on-road traffic, shipping, agriculture and biogenic sources of NMVOCs.

The industrial emissions in the inner domain were obtained from the Spanish Pollutant Release and Transfer Register (PRTR-E; <http://www.prtr-es.es>) which contains emissions from all large industrial installations. The Huelva region has a substantial contribution from industrial emissions with three industrial estates close to the city (Punta del Sebo, Nuevo Puerto and Tartessos) containing a Cu smelter plant, a fertiliser and phosphoric acid production plant, a petroleum refinery and power plants (Fernández-Camacho et al., 2010). There are also substantial industrial emissions in the Algeciras Bay area close to the Gibraltar strait (petroleum refinery, petrochemical processing and power plants). Emissions in this register include  $\text{NO}_x$ , NMVOCs,  $\text{SO}_x$ , CO,  $\text{CO}_2$ ,  $\text{NH}_3$  and  $\text{PM}_{10}$ .  $\text{NH}_3$  emissions reported in this register include those from industrial activities such as fertiliser plants and the chemical industry, and also from large pig and poultry units. NMVOC and fine particulate emissions were speciated for the CB05 chemical mechanism according to EPA speciation profiles (EPA, 2009).  $\text{PM}_{2.5}$  emissions were split into five species:  $\text{PSO}_4$  (primary

sulphate),  $\text{PNO}_3$  (primary nitrate), PEC (Primary Elemental Carbon), POC (Primary Organic Carbon) and PMFINE (other fine PM). As CAMx models organic carbon (OC) as organic mass (OM) a multiplier of 1.2 was used to convert POC to POA (Primary Organic Aerosol).

The on-road traffic emissions were provided from the Spanish National Emission Inventory. The traffic emissions were spatially disaggregated using the road network distribution and the average traffic intensity across that network and were subsequently temporally disaggregated utilising an hourly temporal profile differing for workdays and weekends (Castell et al., 2010a). Chemical speciation of NMVOC and fine particulate emissions for on-road traffic was also conducted using EPA speciation profiles.

Biogenic emissions of NMVOCs with a temporal resolution of one hour were estimated following Guenther et al. (1993, 1995) with emission factors and biomass factors adapted for Mediterranean vegetation species (Castell, 2008) and hourly values of surface air temperature and solar radiation obtained from MM5. Emission and biomass factors were selected according to month and land cover type, using the CORINE (COoRdinate Information on the Environment) land cover maps with a spatial resolution of  $0.0083^\circ$ . Following the Guenther algorithm, NMVOCs are classified into three groups: isoprene, monoterpene and other volatile organic compounds (OVOCs).

Ammonia ( $\text{NH}_3$ ) plays an important role in the formation of secondary inorganic aerosols and as such needs to be adequately included in the emission inventory. According to the 2006 Andalusian Atmospheric Emissions Inventory (COMAAN, 2006), 90.2% of  $\text{NH}_3$  emissions in Andalusia are from agricultural sources with 67.1% of these emissions from fertiliser application and 20.1% from livestock farming. Industrial emissions constitute 2.4% of total  $\text{NH}_3$  emissions. Consequently, in addition to the  $\text{NH}_3$  emissions included from industrial installations and from large pig and poultry units as described above,  $\text{NH}_3$  emissions from fertiliser application to agricultural land were also included in the emission inventory used in this study. The  $\text{NH}_3$  fertiliser application emissions were obtained as municipal totals (COMAAN, 2006) and spatially disaggregated to agricultural land using the CORINE land cover data. Shipping emissions in the inner domain were obtained from the European Pollutant Release and Transfer Register (E-PRTR) diffuse air emission dataset (<http://www.eea.europa.eu/data-and-maps/data/europeanpollutant-release-and-transfer-register-e-prtr-regulation-art-8-diffuse-air-data/>) at 5 km  $\times$  5 km resolution.

### 2.4. Observational data for model evaluation

The simulations were compared against surface-based observational data. Thirteen meteorological stations, twelve belonging to the Meteorological State Agency of Spain (AEMET), and one belonging to the University of Huelva (Valverde del Camino), were used to evaluate the meteorological simulations. These included hourly measurements of 10-m wind speed and wind direction, 2-m air temperature and precipitation. The simulation results of  $\text{PM}_{2.5}$  composition were evaluated using experimental data obtained in four intensive field campaigns performed in September 2008, October 2008, March 2009 and July/August 2009. In each field campaign  $\text{PM}_{2.5}$  samples were collected at three sites (see Fig. 1):

- University Campus ( $37.272^\circ$  N,  $6.925^\circ$  W, 17 m a.s.l.), an urban background site located on the northern side of the city of Huelva.
- CIECEM ( $37.016^\circ$  N,  $6.570^\circ$  W, 15 m a.s.l.), a rural coastal site located at about 30 km SE of the city of Huelva.
- Valverde del Camino ( $37.580^\circ$  N,  $6.756^\circ$  W, 220 m a.s.l.), a rural inland site situated 40 km north of Huelva.



Concentrations of gaseous pollutants ( $\text{NO}_x$ ,  $\text{CO}$ ,  $\text{SO}_2$  and  $\text{O}_3$ ) and particulate matter ( $\text{PM}_{10}$  and  $\text{PM}_{2.5}$ ) were recorded with hourly resolution at the University Campus and CIECEM sites. At Valverde del Camino, ozone concentrations were also monitored. In addition,  $\text{PM}_{10}$  concentrations of black carbon were monitored with ten minute resolution (subsequently averaged to hourly resolution) using a Multi-Angle Absorption Photometer (Thermo<sup>TM</sup>, model CARUSSO 5012). The instrument set up and the used mass-absorption efficiency ( $10.31 \pm 0.25 \text{ m}^2 \text{ g}^{-1}$ ) is described in Fernández-Camacho et al. (2010). The mean ratio of  $\text{PM}_{2.5} \text{ BC}/\text{PM}_{10} \text{ BC}$  ( $0.74 \pm 0.025$ ) was utilised to determine the BC concentration in  $\text{PM}_{2.5}$  (see Fernández-Camacho et al., 2010).

At the three sites, samples of  $\text{PM}_{2.5}$  were collected during day-time (10:00–19:00 GMT) and night-time (22:00–07:00 GMT) using manual gravimetric high volume captors ( $30 \text{ m}^3 \text{ h}^{-1}$ ), and quartz micro-fibre filters (MUNKTELL<sup>®</sup>). The filter measurement times correspond to local time (UTC+1 h in winter and UTC+2 h in summer). Concentrations of secondary inorganic compounds (sulphate, nitrate and ammonium), total carbon, major (Al, Ca, Fe, Na, K and Mn) and trace elements (P, Ti, V, Cr, Mn, Co, Ni, Cu, Zn, As, Se, Rb, Sr, Cd, Sn, Sb, Cs, Ba, Pb, among others) were determined using several techniques (Ion Chromatography, LECO, ICP-OES, ICP-MS) and the procedures described in previous studies (Sánchez de la Campa et al., 2011). These elements allowed the estimation of the contribution of sea salt (Na + Cl + sea salt sulphate) and mineral dust ( $\text{Al}_2\text{O}_3$  +  $\text{SiO}_2$  +  $\text{CaCO}_3$  + Fe + Ti + K + Mn) to the bulk  $\text{PM}_{2.5}$  concentrations. Sea salt sulphate (ss-sulphate) was determined using Na/sulphate ratio in sea water, and their concentrations were extracted from bulk sulphate concentrations. Herein after, we will refer to sulphate as the fraction that remained after subtracting the ss-sulphate. Details on the indirect determinations of  $\text{SiO}_2$ ,  $\text{CaCO}_3$  are provided by Querol et al. (2001).

## 2.5. Evaluation statistics

The statistical metrics used to evaluate the comparison of modelled data against observational data are Mean Bias (MB), Normalized Mean Bias (NMB) and the coefficient of determination ( $r^2$ ). In addition, we present values of the Mean Fractional Bias (MFB) and Mean Fractional Error (MFE) proposed by Boylan and Russell (2006). They suggested that model evaluation should be compared against the mean of both observed and modelled concentrations due to uncertainties in both categories. This is particularly the case when considering aerosol concentrations which are known to be subject to substantial uncertainties dependent on aerosol component and measurement technique. All evaluation statistics have been calculated using modelled concentrations from the inner domain.

## 2.6. Synoptic meteorology during campaigns

### 2.6.1. Campaign 1: 12–24 September 2008

Synoptic meteorology during campaign 1 was characterized by a high frequency of low pressure systems moving west-to-east across Spain. From Sept 12 to 15, the Iberian Peninsula was under the influence of the Azores high (North Atlantic anticyclone). From Sept 16 to 24 four depressions crossed from the Atlantic to the Mediterranean through Southern Spain, resulting in frequent Western airflows and rain over the study region.

### 2.6.2. Campaign 2: 6–23 October 2008

Synoptic meteorological conditions varied between the passage of cold fronts and advections of Saharan dust over southern Spain. From Oct 19 to 23 southern air-flows and rain were prompted by depressions crossing from the Atlantic to the Mediterranean over Gibraltar.

### 2.6.3. Campaign 3: 9–22 March 2009

Campaign 3 was dominated by winter anticyclonic conditions. March 2009 was unseasonably warm and dry and there was no precipitation recorded during this campaign. During Mar 9–12, the Azores high extended and moved towards central Europe. These weak pressure gradient conditions favoured the development of local circulations. This was followed by transport of air mass from Africa during Mar 13–16. On Mar 17 the arrival of a cut-off low to the western Mediterranean brought cold air and higher wind speeds, thereby renovating the air mass. On Mar 19 synoptic conditions favouring dust transport from Africa returned until the end of the campaign.

### 2.6.4. Campaign 4: 9 July–3 August 2009

Campaign 4 in general corresponded to a typical summer situation. During July 9–16 weak pressure gradient conditions and the development of the Iberian thermal low favoured local circulations. On Jul 17 a cold trough passed over the peninsula, introducing a synoptic northerly wind and renovating the air mass. In the following two weeks, the synoptic conditions varied between increased atmospheric stability and African air mass intrusions affecting the study area (18–22, 26 and 28–31 July) broken in between by the passage of cold troughs (Jul 23) and fronts (Jul 27, Aug 1) renovating the air mass.

## 3. Results and discussion

### 3.1. Meteorology

The evaluation of the meteorological model against the 13 meteorological stations showed that the model captured the diurnal variability, seasonal changes and the large spatial variability in this complex area. The meteorological stations located closest to the measurement sites were Valverde (co-located with Valverde measurement site), Ronda Este (located 2 km from University Campus) and El Arenosillo (located 18 km from CIECEM). Example observed and simulated wind speed and wind direction data is shown in Fig. 2 for these three meteorological stations. In general the meteorological model had a tendency to slightly underpredict the wind speed in inland areas and overpredict the wind speed during certain periods in coastal areas. For example, during Campaign 3 at the coastal site of El Arenosillo (Fig. 2C1), simulated wind speed was similar to observations during the first week while overestimating observations in the second week. Mean biases for simulated temperature across the four campaign periods ranged between  $-0.9^\circ\text{C}$  and  $0.9^\circ\text{C}$  for the 13 different stations. Simulated wind speed biases for the four campaign periods were between  $-0.5 \text{ m s}^{-1}$  and  $1.7 \text{ m s}^{-1}$  for the different stations.

### 3.2. Ozone

The time series of simulated against observed ozone for the urban site for Campaign 4 is shown in Fig. 3, demonstrating that the model captures the behaviour of the ozone concentrations. The mean bias for ozone for Campaign 4 was  $-3.6 \text{ ppb}$ . Comparisons were also conducted for the rest of the campaigns and similar results were found; the mean biases for Campaign 1, 2, and 3 were  $-0.8 \text{ ppb}$ ,  $0.3 \text{ ppb}$  and  $-7.2 \text{ ppb}$ , respectively.

### 3.3. Chemical characterisation of $\text{PM}_{2.5}$

The mean composition of  $\text{PM}_{2.5}$  during the four campaigns was analysed for each of the three sampling sites (see Table 1A). Concentrations of  $\text{PM}_{2.5}$  at the rural inland (Valverde) and rural coastal (CIECEM) sites ( $\sim 20 \mu\text{g m}^{-3}$ ) account for  $\sim 80\%$  of those registered

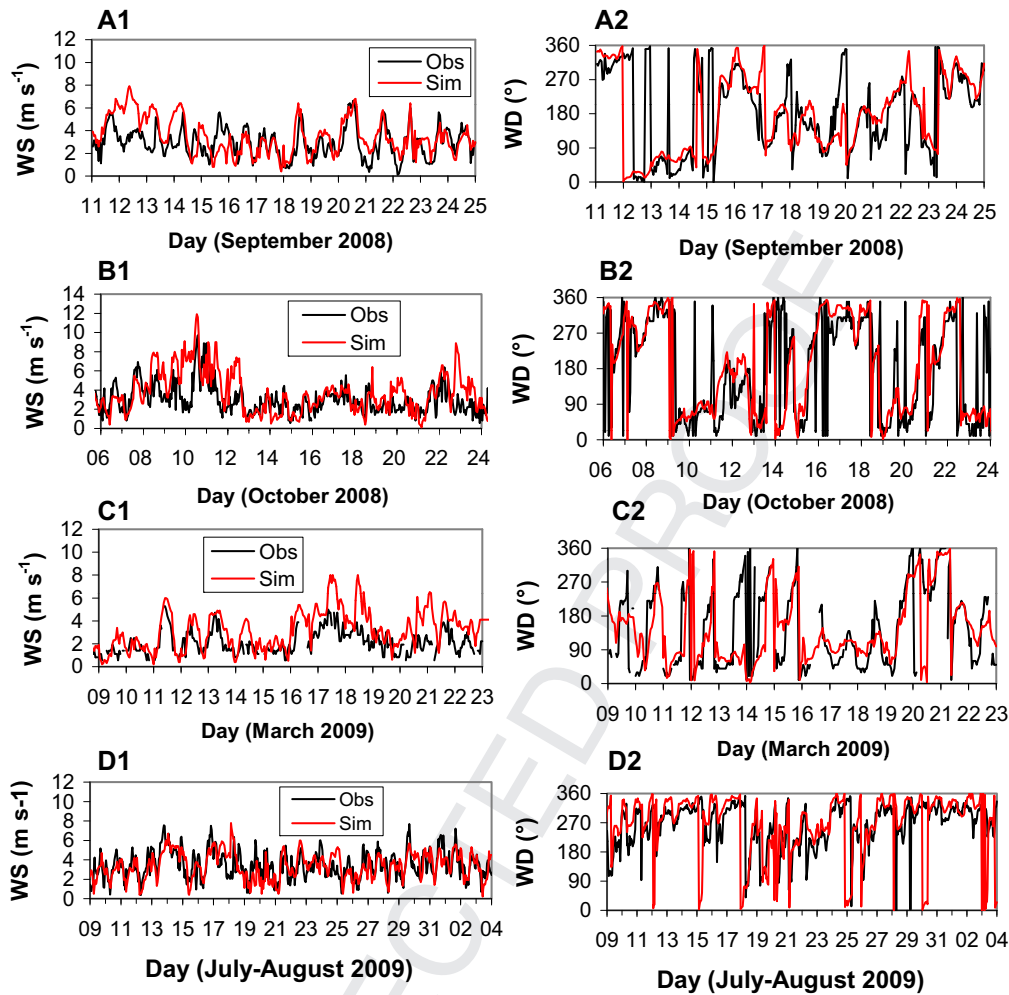


**Fig. 2.** Observed and simulated wind speed (WS) and wind direction (WD) during Campaign 1, 2, 3 and 4 at Valverde (A & D), Huelva, Ronda Este (B), and El Arenosillo (C), respectively.

at University Campus urban background site ( $26 \mu\text{g m}^{-3}$ ). This evidences the already described high background of  $\text{PM}_{2.5}$  in the study region (Valverde and CIECEM are 30–40 km distant from the industrial area). This high background is mostly due to the relatively homogeneous spatial distribution of mineral dust, organic matter, sulphate and ammonium, whose concentrations are within the ranges  $4.0\text{--}7.0 \mu\text{g m}^{-3}$ ,  $4.0\text{--}6.0 \mu\text{g m}^{-3}$ ,  $2.5\text{--}3.0 \mu\text{g m}^{-3}$  and  $0.7\text{--}0.8 \mu\text{g m}^{-3}$ , respectively, across the three sites.

The composition of  $\text{PM}_{2.5}$  exhibits some features to be considered before proceeding with the model evaluation; a significant

fraction of sulphate, and most of nitrate, is not present as ammonium salts. The concentrations of sulphate and nitrate versus ammonium expressed in equivalents are shown in Fig. 4A and B. Observe how, although  $\text{SO}_4^{2-}$  and  $\text{NH}_4^+$  show a high correlation there is a clear excess of  $\text{SO}_4^{2-}$ , probably occurring as Na and/or Ca salts. In contrast, nitrate shows a poor correlation and deficit with ammonium during the campaigns 1, 2 and 4, performed in warm and hot seasons (Sept, Oct and Jul), when temperatures ranged between  $13^\circ\text{C}$  and  $40^\circ\text{C}$ . Only during Campaign 3 (March 2009) do we observe a significant correlation and availability of ammonium

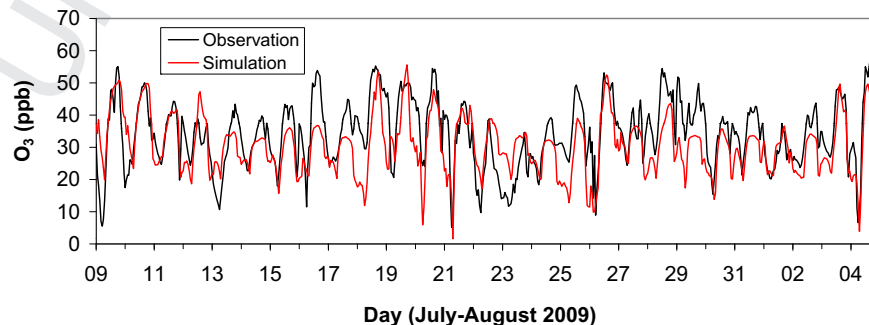


**Fig. 3.** Observed and simulated ozone concentration at University Campus during Campaign 4.

**Table 1**

A) Mean composition of PM<sub>2.5</sub> during the four field campaigns at the three sites (University Campus, Valverde and CIECEM) expressed in  $\mu\text{g m}^{-3}$  and as % of total PM<sub>2.5</sub>.  $\Sigma$ : sum of the determined aerosol components. B) Segregation of sulphate and nitrate in their ammonium salts: ammonium sulphate (a-sulphate), non-ammonium sulphate (na-sulphate), ammonium nitrate (a-nitrate), non-ammonium nitrate (na-nitrate).

	Univ. C $\mu\text{g m}^{-3}$	Urban %	Valverde $\mu\text{g m}^{-3}$	Rural inland %	CIECEM $\mu\text{g m}^{-3}$	Coastal %
<b>A)</b>						
PM <sub>2.5</sub>	26.05		21.56		19.98	
OM + BC	6.66	26	7.63	35	4.47	22
OM	6.12	23	4.67 <sup>a</sup>	22	4.14 <sup>b</sup>	21
BC	0.54	2	0.37 <sup>a</sup>	2	0.36 <sup>b</sup>	2
SO <sub>4</sub> <sup>2-</sup>	2.65	10	2.50	12	2.87	14
NO <sub>3</sub> <sup>-</sup>	1.20	5	0.70	3	0.68	3
NH <sub>4</sub> <sup>+</sup>	0.83	3	0.73	3	0.70	3
Dust	6.89	26	4.35	20	4.62	23
Sea salt	1.29	5	0.95	4	1.24	6
$\Sigma$ components	19.52	75	16.86	78	14.24	74
<b>B)</b>						
Sulphate	2.65		2.50		2.87	
a-sulphate	2.01	76	1.84	73	1.81	63
na-sulphate	0.64	24	0.66	27	1.06	37
Nitrate	1.20		0.70		0.68	
a-nitrate	0.25	21	0.11	16	0.04	6
na-nitrate	0.95	79	0.59	84	0.64	94

<sup>a</sup> The segregation between OM and BC was only performed in Valverde during Campaign 3.

<sup>b</sup> The segregation between OM and BC was performed in CIECEM during Campaigns 1–3.

(Fig. 4B) resulting in the formation of significant amounts of ammonium nitrate. This is attributed to the lower temperatures recorded during this campaign, which decreased down to 8 °C. We then estimated the amount of sulphate and nitrate presents as ammonium salts (ionic balance): ammonium-sulphate (a-sulphate), non-ammonium sulphate (na-sulphate), ammonium nitrate (a-nitrate) and non-ammonium nitrate (na-nitrate). Mean values are shown in Table 1B: as an average, 63–76% of sulphate is present as a-sulphate across the three sites, whereas only 6–21% of nitrate is present as a-nitrate. The moderate to high correlation observed between na-nitrate and the excess of Na versus the Na/Cl ratio in sea salt (Fig. 4C), points to the formation of Na-nitrate by reaction of nitric acid with sea salt (Harrison and Pio, 1983).

These features we observed in the study region (high contributions of mineral dust, nitrate predominantly as non-ammonium nitrate and a significant load of non-ammonium sulphate) are considered typical features of southern Europe, not typically observed in central and northern Europe (Rodríguez et al., 2007a,b).

### 3.4. PM<sub>2.5</sub> ammonium

The time series of simulated against observed PM<sub>2.5</sub> NH<sub>4</sub> concentrations for the three different measurement sites and for the four campaigns are shown in Fig. 5, while evaluation statistics are provided in Table 2. Performance varies between the four campaigns and between sites; generally the model captures the

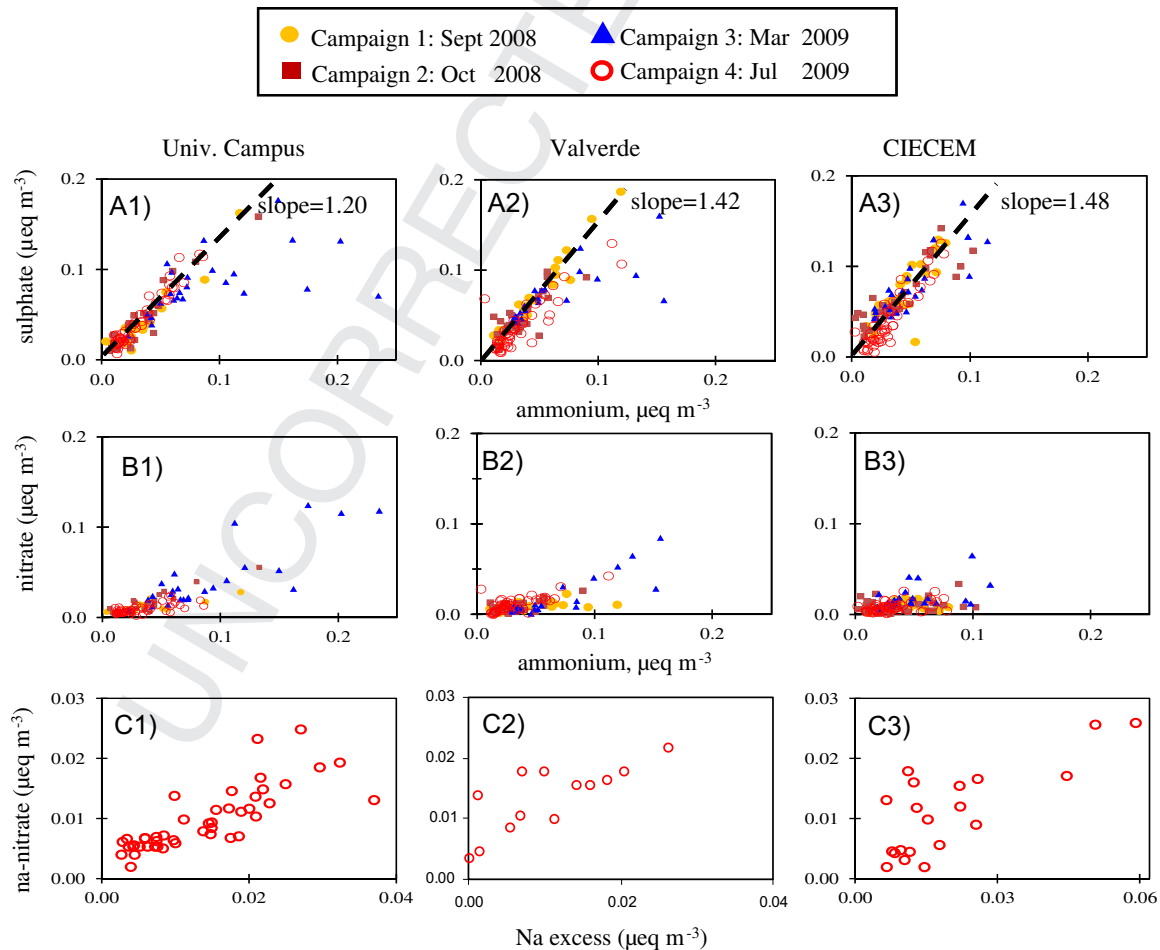


**Fig. 4.** A) Sulphate versus ammonium scatter plot, B) Nitrate versus ammonium scatter plot C) Non-ammonium nitrate (na-nitrate) versus the excess of Na with respect to the Na/Cl sea salt ratio.

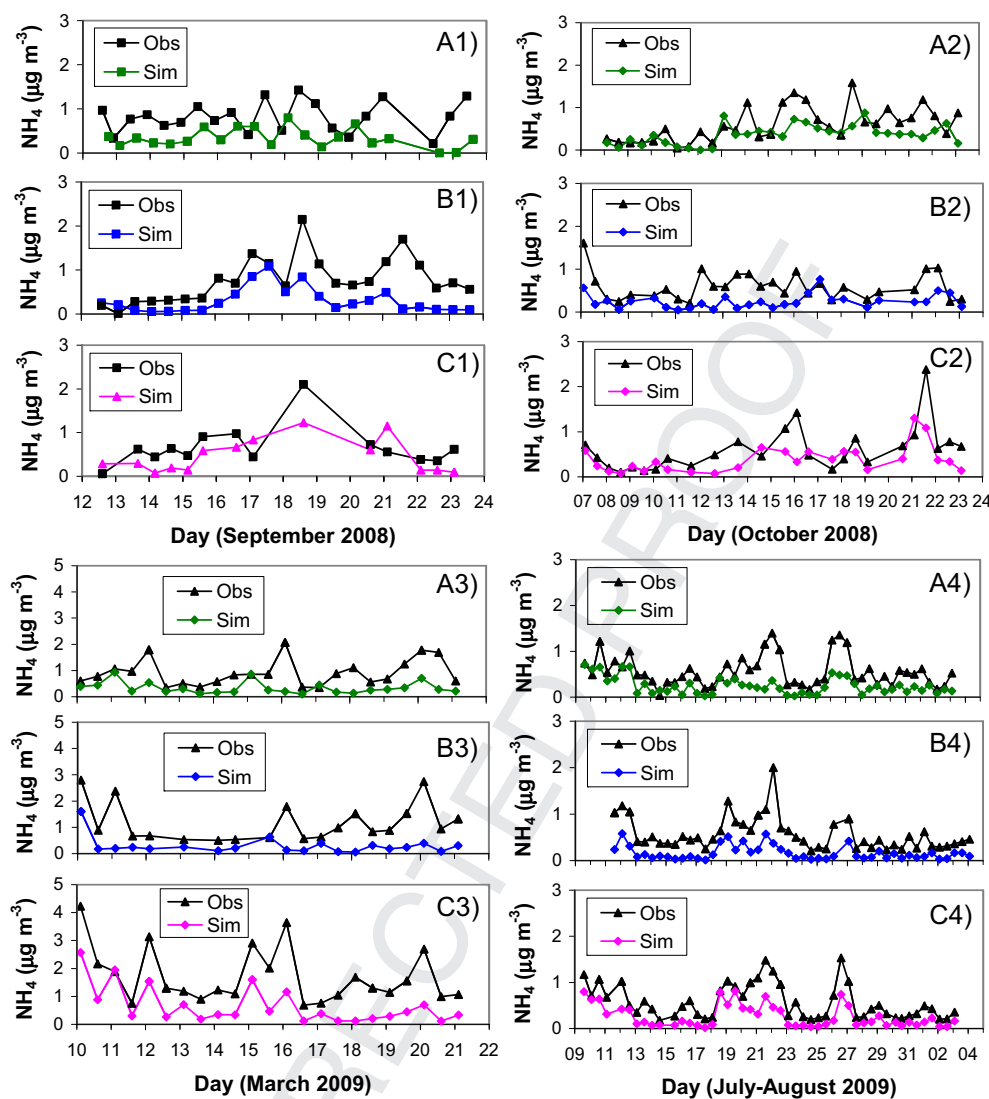


Fig. 5. Observed and simulated PM<sub>2.5</sub> NH<sub>4</sub> concentrations at A) CIECEM, B) Valverde and C) University Campus during the four campaigns (1–4).

Table 2

Statistical metrics for PM<sub>2.5</sub> NH<sub>4</sub> concentrations at all sites. SM (Simulated mean), OM (Observed mean), MB (Mean Bias), NMB (Normalized Mean Bias),  $r^2$  (Coefficient of determination).

	SM ( $\mu\text{g m}^{-3}$ )	OM ( $\mu\text{g m}^{-3}$ )	MB ( $\mu\text{g m}^{-3}$ )	NMB (%)	$r^2$
<b>Campaign 1</b>					
CIECEM	0.33	0.81	−0.5	−59	0.01
Univ. Campus	0.45	0.67	−0.2	−32	0.50
Valverde	0.31	0.80	−0.5	−59	0.42
<b>Campaign 2</b>					
CIECEM	0.33	0.61	−0.3	−46	0.22
Univ. Campus	0.39	0.61	−0.2	−35	0.62
Valverde	0.24	0.59	−0.4	−48	0.14
<b>Campaign 3</b>					
CIECEM	0.32	0.91	−0.6	−65	0.05
Univ. Campus	0.64	1.71	−1.1	−63	0.60
Valverde	0.28	1.17	−0.9	−75	0.23
<b>Campaign 4</b>					
CIECEM	0.25	0.56	−0.3	−55	0.38
Univ. Campus	0.26	0.57	−0.3	−55	0.72
Valverde	0.16	0.56	−0.4	−65	0.69

variability in the concentrations but tends to underestimate the magnitude of the PM<sub>2.5</sub> NH<sub>4</sub> concentrations, with a larger underestimation in the winter-time. Correlations between simulated and observed data are highest for the urban site, University Campus ( $r^2 = 0.50$ – $0.72$ ), followed by Valverde ( $r^2 = 0.14$ – $0.69$ ) and the rural coastal site, CIECEM ( $r^2 = 0.01$ – $0.38$ ). Normalized Mean Bias values are similar for CIECEM and University Campus (ranging between  $-32\%$  and  $-65\%$ ) while Valverde shows NMB values of  $-48\%$  to  $-75\%$ .

Boylan and Russell (2006) introduced the concept of 'bugle plots' which can be used to examine the performance of a model for different periods or locations, indicating how mean fractional biases or error vary with concentration. The average concentration plotted on the x-axis is the average of the mean observed and mean simulated concentration. Boylan and Russell (2006) also proposed performance criteria (MFB  $\leq \pm 60\%$  and MFE  $\leq +75\%$ ) and performance goals for MFB ( $\leq \pm 30\%$ ) and MFE ( $\leq \pm 30\%$ ). Comparing the PM<sub>2.5</sub> NH<sub>4</sub> campaign values to the performance criteria and goal for MFB (Fig. 6a) demonstrates that the majority of the sites and comparison periods met the MFB criteria while half of the values met the performance goal. With respect to MFE (Fig. 6b), the majority of the sites and comparison periods met the performance



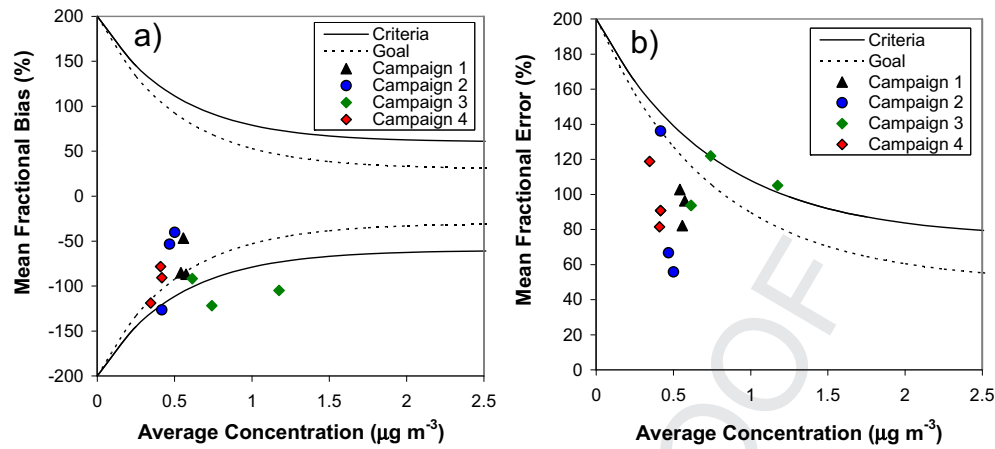


**Fig. 6.** a) Mean fractional bias and b) mean fractional error for  $\text{PM}_{2.5} \text{NH}_4$  concentrations during the four campaigns. The average concentration plotted on the x-axis is the average of the observed and simulated concentration.

goal with only one site during Campaign 3 not meeting the performance criteria.

### 3.5. $\text{PM}_{2.5}$ sulphate

The simulated  $\text{PM}_{2.5} \text{SO}_4$  concentrations were first compared against measurement observations of total non-marine sulphate. Evaluation statistics for this comparison are provided in Table 3A. However, as the CAMx model version used in this study (v4.51) only simulates the formation of ammonium sulphate, secondly, the simulated  $\text{PM}_{2.5} \text{SO}_4$  concentrations were compared against measurement observations of sulphate as ammonium sulphate (Table 3B, Fig. 7).

Examining the evaluation statistics for these two comparisons (Table 3A and B) quantifies the improvement in the model-measurement comparison and demonstrates the importance of comparing the same components of particulate sulphate in the model evaluation rather than comparing simulations with measurements of total non-marine sulphate. As can be expected, the Mean Bias and the Normalized Mean Bias values are seen to improve substantially; the mean NMB for all campaigns and sites is reduced from  $-68\%$  to  $-55\%$ . The correlation also substantially

improves for some sites and campaigns while remaining similar or slightly reducing for others.

The following discussion refers to the model comparison with the measurement observations of sulphate as ammonium sulphate (Table 3B). As for  $\text{PM}_{2.5} \text{NH}_4$ , the model captures the variability in the concentrations but tends to underestimate the magnitude of the  $\text{PM}_{2.5} \text{SO}_4$  concentrations. Correlations are highest for the summertime campaigns (mean  $r^2$  values for Campaign 1, 2 and 4 are 0.41, 0.23 and 0.62, respectively) and lowest for the wintertime campaign (mean  $r^2 = 0.08$ ). Normalized Mean Bias values are greatest for the wintertime campaign ( $-74\%$ ) and lowest for Campaign 1 ( $-42\%$ ). Examining the bugle plots for sulphate demonstrates that just under half of the sites and comparison periods met the MFB criteria (Fig. 8a) while all of the sites except one met the MFE criteria in Campaigns 1, 2 and 4 (Fig. 8b). None of the sites during Campaign 3 met the criteria for MFB or MFE, again demonstrating the poorer performance during the wintertime campaign.

In general in this region, sulphate concentrations are at a maximum in summer due to enhanced photochemistry (Rodríguez et al., 2007a). However, winter anticyclonic conditions, such as those experienced during Campaign 3, can lead to a substantial

**Table 3**  
Statistical metrics for  $\text{PM}_{2.5} \text{SO}_4$  concentrations at all sites. SM (Simulated mean), OM (Observed mean), MB (Mean Bias), NMB (Normalized Mean Bias),  $r^2$  (Coefficient of determination).

	SM ( $\mu\text{g m}^{-3}$ )	A: Total non-marine sulphate concentrations				B: Ammonium sulphate concentrations			
		OM ( $\mu\text{g m}^{-3}$ )	MB ( $\mu\text{g m}^{-3}$ )	NMB (%)	$r^2$	OM ( $\mu\text{g m}^{-3}$ )	MB ( $\mu\text{g m}^{-3}$ )	NMB (%)	$r^2$
<b>Campaign 1</b>									
CIECEM	1.33	3.53	−2.2	−62	0.26	2.09	−0.8	−36	0.17
Univ. Campus	1.08	2.16	−1.1	−50	0.58	1.72	−0.6	−38	0.55
Valverde	0.99	3.18	−2.2	−70	0.48	2.15	−1.1	−53	0.53
<b>Campaign 2</b>									
CIECEM	0.79	2.96	−2.1	−72	0.16	1.62	−0.8	−51	0.27
Univ. Campus	0.85	2.46	−1.6	−66	0.09	1.56	−0.7	−45	0.27
Valverde	0.62	2.21	−1.6	−71	0.03	1.54	−0.9	−60	0.15
<b>Campaign 3</b>									
CIECEM	0.75	3.76	−3.0	−80	0.07	2.40	−1.6	−69	0.09
Univ. Campus	0.90	4.19	−3.3	−77	0.07	3.64	−2.7	−75	0.16
Valverde	0.64	3.53	−2.9	−81	0.003	2.77	−2.1	−77	0.01
<b>Campaign 4</b>									
CIECEM	0.81	2.02	−1.2	−57	0.59	1.43	−0.6	−43	0.48
Univ. Campus	0.70	2.13	−1.4	−65	0.75	1.52	−0.8	−54	0.72
Valverde	0.45	1.73	−1.2	−66	0.61	1.41	−0.9	−61	0.69

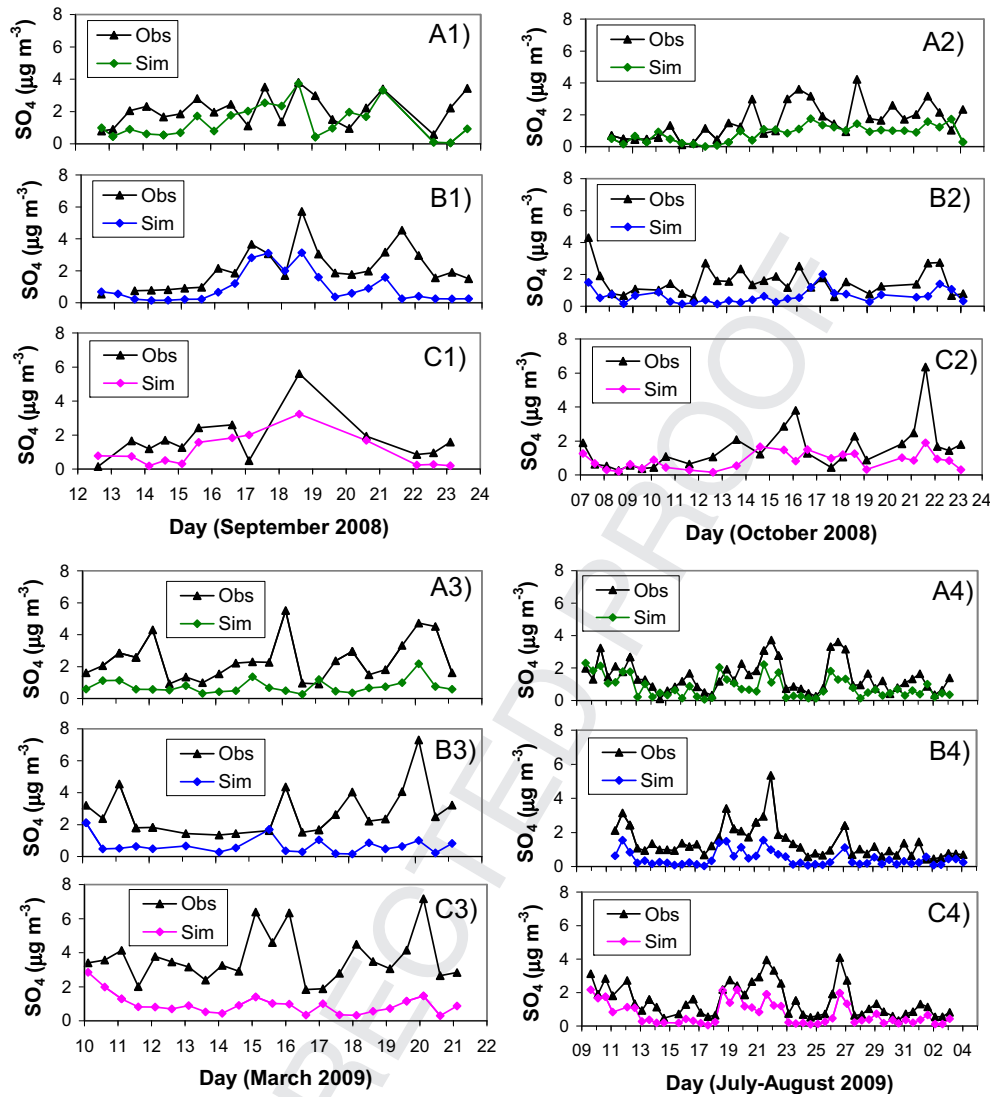


Fig. 7. Observed and simulated  $PM_{2.5}$   $SO_4$  concentrations (as ammonium sulphate) at A) CIECEM, B) Valverde and C) University Campus during the four campaigns (1–4).

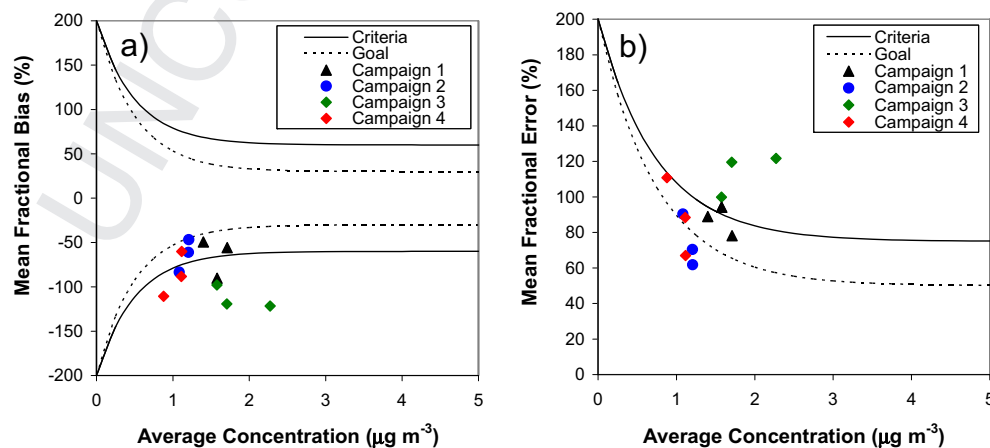


Fig. 8. a) Mean fractional bias and b) mean fractional error for  $PM_{2.5}$   $SO_4$  concentrations (as ammonium sulphate) during the four campaigns. The average concentration plotted on the x-axis is the average of the observed and simulated concentration.

**Table 4**

Mean concentrations of observed Total PM<sub>2.5</sub> nitrate and ammonium nitrate (a-nitrate) and simulated ammonium nitrate at all sites, plus the estimated ratio of measured ammonium nitrate/Total PM<sub>2.5</sub> nitrate. SM (simulated mean), OM (observed mean).

	PM <sub>2.5</sub> nitrate OM (μg m <sup>-3</sup> )	Ammonium-nitrate OM (μg m <sup>-3</sup> )	Ammonium-nitrate SM (μg m <sup>-3</sup> )	Ammonium nitrate/PM <sub>2.5</sub> nitrate (%) <sup>a</sup>
<b>Campaign 1</b>				
CIECEM	0.60	0.00	0.02	0
Univ. Campus	0.73	0.07	0.16	9
Valverde	0.48	0.00	0.01	0
<b>Campaign 2</b>				
CIECEM	0.60	0.00	0.20	0
Univ. Campus	1.19	0.06	0.29	5
Valverde	0.52	0.01	0.05	3
<b>Campaign 3</b>				
CIECEM	1.20	0.03	0.21	2
Univ. Campus	2.79	0.79	0.94	28
Valverde	0.90	0.17	0.01	19
<b>Campaign 4</b>				
CIECEM	0.51	0.06	0.00	12
Univ. Campus	0.61	0.01	0.00	2
Valverde	0.66	0.08	0.00	12

<sup>a</sup> From observations.

increase in aerosol concentrations. Pey et al. (2010) found that winter anticyclonic periods were responsible for the highest concentrations in PM<sub>10</sub>, PM<sub>2.5</sub> and PM<sub>1</sub> fractions in comparison with other meteorological scenarios considered. In this study, the highest sulphate concentrations were observed during the wintertime campaign; the mean concentration at University Campus (3.64 μg m<sup>-3</sup>) was more than double that of the summertime campaign (1.52 μg m<sup>-3</sup>) and the maximum concentration (7.17 μg m<sup>-3</sup>) was also substantially higher than in the summertime campaign (4.09 μg m<sup>-3</sup>).

Poorer performance for sulphate episodes in wintertime compared to summertime has been documented in other studies (e.g. Beekmann et al., 2007; Schaap et al., 2011; Pay et al., 2011), and may in part be due to difficulties in the meteorological simulation of these winter-time pollution episodes as well as issues of oxidant availability.

### 3.6. PM<sub>2.5</sub> nitrate

Simulated nitrate was zero or near zero for all sites in Campaign 1 and 4. Only during the wintertime campaign at University Campus were sizeable amounts of nitrate simulated (Table 4, Fig. 9). Although the ISORROPIA aerosol thermodynamic module utilised in CAMx for partitioning of inorganic aerosols includes the interactions between sodium and chloride and the

other major inorganic aerosol species (Nenes et al., 1998) our current model implementation does not include sea-salt aerosol (SSA) emissions. Consequently the simulated nitrate concentrations presented here arise solely from the formation of ammonium nitrate.

As shown in Section 3.3, the estimated contribution of ammonium nitrate to total PM<sub>2.5</sub> nitrate in the observational data was also found to be very small. Mean concentrations of ammonium nitrate during the summertime campaigns at the three sites were estimated as 0–0.08 μg m<sup>-3</sup> (Table 4) resulting in a mean ratio of ammonium nitrate/total PM<sub>2.5</sub> nitrate during these summertime periods of only 4–5%. Only during the wintertime period did ammonium nitrate form a larger (but still low) contribution to the particulate nitrate; mean concentrations were between 0.03 and 0.79 μg m<sup>-3</sup> (Table 4), resulting in a mean ratio of ammonium nitrate/total PM<sub>2.5</sub> nitrate of 2–28%. This is attributed to the colder temperatures and higher humidities during Campaign 3 favouring the formation of particulate ammonium nitrate in the NH<sub>3</sub>–HNO<sub>3</sub>–NH<sub>4</sub>NO<sub>3</sub> equilibrium.

The importance of considering the composition of particulate nitrate in the model evaluation is demonstrated by the comparison of simulated values of ammonium nitrate versus total PM<sub>2.5</sub> nitrate observations and versus estimated ammonium nitrate observations for University Campus during Campaign 3 (Fig. 9). Estimated ammonium nitrate observations were close to zero for much of the campaign apart from the nights 11–12 Mar and 15–16 Mar. The CAMx simulated values of ammonium nitrate capture these observations and the zero or near-zero ammonium nitrate concentrations during many periods (e.g. 17–21 Mar).

Considering the dominance of non-ammonium nitrate in our measured PM<sub>2.5</sub> nitrate composition, future improvements to our model simulations would include the implementation of sea-salt aerosol emissions to incorporate the formation of sodium nitrate and indeed a CAMx preprocessing utility to generate sea-salt aerosol emissions is now available. Athanasopoulou et al. (2008) have also demonstrated the importance of including SSA emissions, particularly in polluted coastal areas and quantify both the direct (addition of sea-salt) and indirect effect (the heterogeneous reaction of sodium chloride with sulphuric and nitric acid) of SSA. They found SSA to contribute between 20–60% of PM<sub>10</sub> and around 10% of PM<sub>2.5</sub> concentrations at coastal sites in their study area (Attica peninsula, Greece).

### 3.7. PM<sub>2.5</sub> black carbon: high temporal resolution

A novel part of the project included high temporal resolution (10 min mean) measurements of black carbon (BC), measured simultaneously at the urban and rural sites. The PM<sub>2.5</sub> BC concentrations were compared against simulated primary elemental

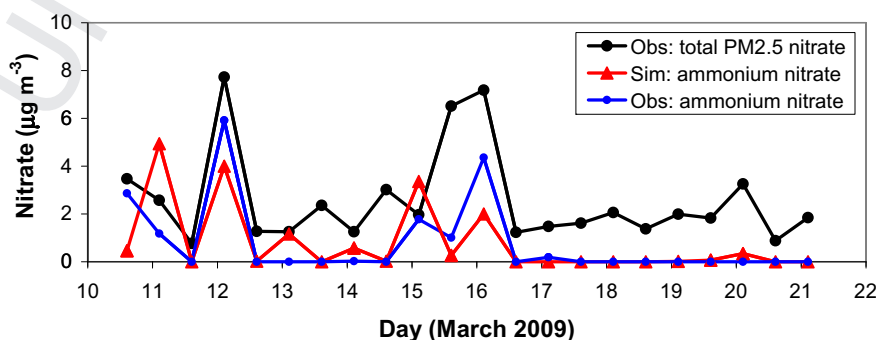
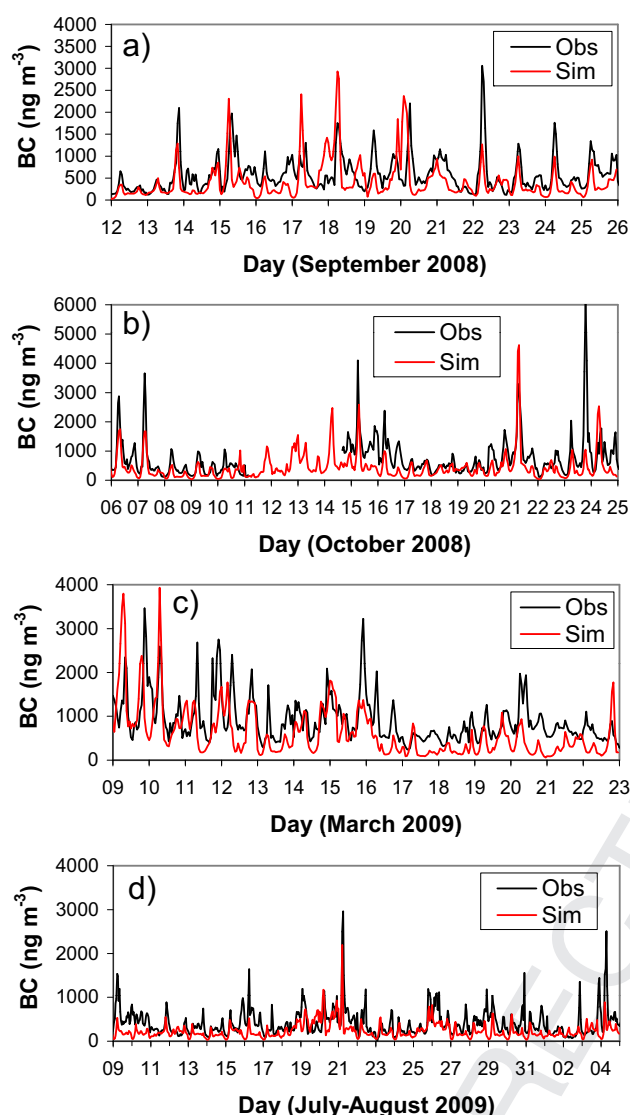


Fig. 9. Observed total PM<sub>2.5</sub> nitrate, observed and simulated ammonium nitrate concentrations at University Campus during Campaign 3.



**Fig. 10.** Observed BC ( $PM_{2.5}$ ) and simulated  $PM_{2.5}$  PEC concentrations at University Campus during all campaigns.

carbon (PEC) concentrations. The model performed well in capturing the hourly, daily and seasonal variability at the urban site (University Campus) (Fig. 10) with  $r^2$  values varying between 0.19 and 0.41 for the four campaigns (Table 5). In general the model tended to underestimate the concentrations slightly with normalised mean bias ranging from –27 to –52%.

**Table 5**

Statistical metrics for observed BC ( $PM_{2.5}$ ) and simulated  $PM_{2.5}$  PEC at University Campus and CIECEM. SM (Simulated mean), OM (Observed mean), MB (Mean Bias), NMB (Normalized Mean Bias),  $r^2$  (Coefficient of determination).

	SM ( $ng\ m^{-3}$ )	OM ( $ng\ m^{-3}$ )	MB ( $ng\ m^{-3}$ )	NMB (%)	$r^2$
<b>University Campus</b>					
Campaign 1	428	585	–157	–27	0.19
Campaign 2	418	749	–331	–44	0.41
Campaign 3	614	908	–369	–52	0.27
Campaign 4	249	416	–167	–40	0.29
<b>CIECEM</b>					
Campaign 1	105	279	–174	–62	0.14
Campaign 2	187	298	–112	–37	0.01
Campaign 3	148	513	–380	–81	0.10

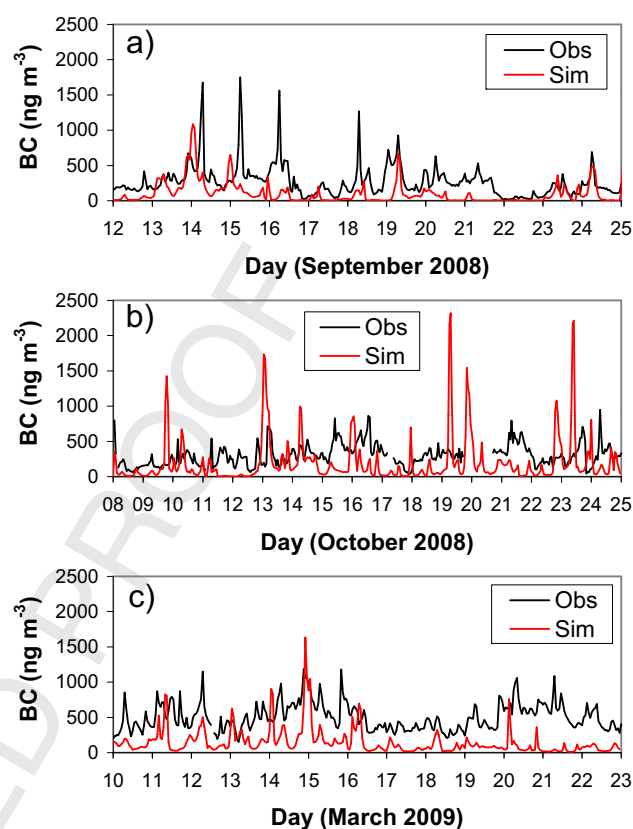


**Fig. 11.** Observed BC ( $PM_{2.5}$ ) and simulated  $PM_{2.5}$  PEC concentrations at CIECEM during Campaign 1, 2 and 3. No measurement data available for Campaign 4.

The model did not perform so well at the rural site (CIECEM) (Fig. 11) with  $r^2$  values varying between 0.01 and 0.14 for the three campaigns (Table 5). The underestimation of concentrations was more pronounced, with the NMB ranging from –37 to –81%. The emission inventory employed in this study is better characterized for the urban than for the rural areas in terms of elemental carbon. There is a detailed inclusion of on-road traffic emissions but there are no agricultural machinery emissions and currently no residential combustion emissions in the inventory, so this can help explain the discrepancy between the measurements and simulations at the rural site. There may be some contribution from residential combustion sources in the cold season in our study area and this would be expected to be a larger contribution in rural areas, however on average we would expect the contribution from this source sector to be much less than in northern Europe. Tsyro et al. (2007) modelled elemental carbon across Europe with the EMEP model and found an overestimation of modelled EC for Nordic sites and an underestimation for sites in Central and Southern Europe. They also highlight the uncertainties in EC emissions from residential combustion as a possible cause for the discrepancies between model estimates and observations, not only due to emission factors but also due to the spatial and temporal disaggregation of these emissions.

### 3.8. $PM_{2.5}$ organic carbon

The model results compared against derived measurements of organic carbon (see Section 2.4) are shown in Fig. 12. As CAMx models organic carbon (OC) as organic mass (OM) the model OM results were converted back to OC using a multiplier of 1/1.2 for



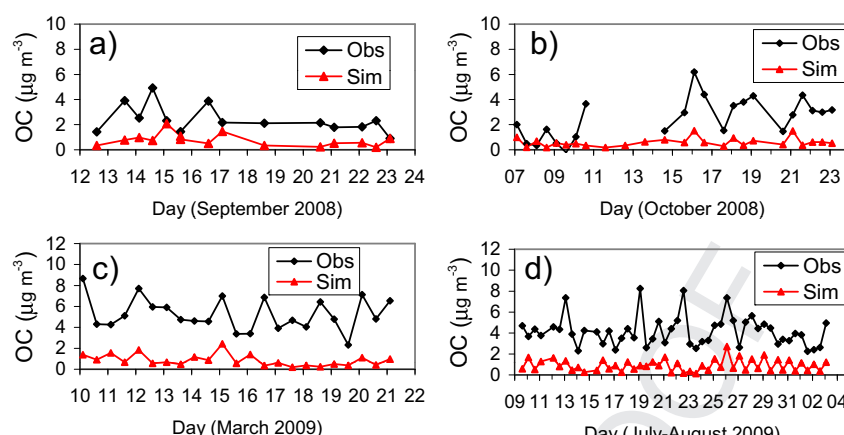


Fig. 12. Observed and simulated PM<sub>2.5</sub> OC concentrations at University Campus during all campaigns.

modelled primary OM and multiplier of 1/1.8 for modelled Secondary Organic Aerosol, following Gaydos et al. (2007). The model clearly underestimates organic carbon in all four campaigns and as for other components the strongest underestimation is observed during Campaign 3. This underestimation of organic carbon has also been found in other studies (e.g. Morris et al., 2006; Pun et al., 2009; Li et al., 2011). Pun et al. (2009) underpredicted OM by about 60%. Simpson et al. (2007) conducted a modelling study of carbonaceous aerosol over Europe with the EMEP model and found significant underprediction of total carbon (TC) in southern Europe, particularly in wintertime, while much better agreement was found for northern Europe. Although many model improvements have been made in recent years, there is still large uncertainty in the simulation of organic and in particular secondary organic aerosol components of PM<sub>2.5</sub> (e.g. Solazzo et al., 2012).

### 3.9. Scenarios of regional pollution episodes

Although a detailed description of the meteorological patterns that influence the dispersion and transport of secondary aerosols in the region is out of the scope of this paper, some important issues will be highlighted. An analysis of the model simulations evidences that there are different scenarios in which the regional transport of pollutants occurs. The sulphate events occurring between 18 and 22 July 2009 are used as examples. The time series of simulated (1 h time resolution) and measured (9 h time resolution) sulphate concentrations at Valverde (rural), Univ. Campus (urban) and CIECEM (coastal) sites are shown in Fig. 13 while simulated surface concentrations of sulphate are shown in Fig. 14.

#### 3.9.1. Events linked to emissions from southern Spain

Emissions from the industrial estates of Huelva and Algeciras Bay clearly have an influence on the air quality of the region. The typical alternation between Easterly–Westerly winds in the Gibraltar strait influence the dispersion of the Algeciras Bay plume. Under Easterly winds, high concentrations of sulphate have been observed at the coastal CIECEM site associated with the arrival of the Algeciras Bay plume (e.g. Fig. 14A). Similarly, the Huelva plume frequently contributes to high sulphate concentrations at Huelva, CIECEM and Valverde sites (e.g. Fig. 14B). The dispersion of the Huelva plume is also highly influenced by the coastal breeze development, which, especially in summer, results in the inland transport of the industrial plume along the Guadalquivir river basin, reaching in some cases Seville city.

#### 3.9.2. Events linked to offshore emissions

Sulphate events due to the shoreward transport of the plume of ships from offshore have also been observed during the periods simulated in the four campaigns of this study. These plumes typically arrive from the corridor that expands from the Strait of Gibraltar to the San Vincent cape, which further expands along the coast of Portugal northward. About 90,000 ships cross the Strait of Gibraltar every year (Moreno-Gutiérrez et al., 2012). High concentrations of sulphate in this strait due to ship emissions are clearly observed in the simulations. This air mass enriched in sulphate is frequently transported northward to the shore, when southern winds blow (e.g. prompted by a low pressure at the west of Portugal) leading to increased sulphate concentrations in CIECEM-coastal site and inland sites (e.g. Fig. 14C). The analysis of the simulated fields also indicates that emissions from Portugal may easily mix with ship emissions before arriving to SW Spain. The inland transport of these various contributing emission sources can lead to a significant accumulation and formation of pollutants.

These events evidence the complexity of the air management in the region, where offshore emissions from shipping, from SW Spain

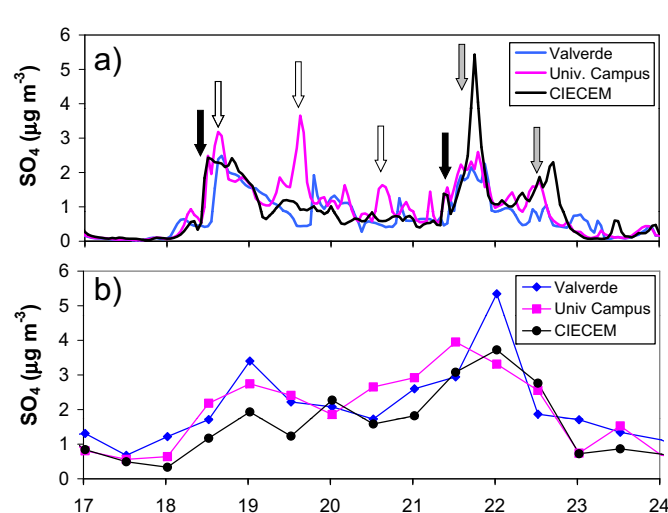
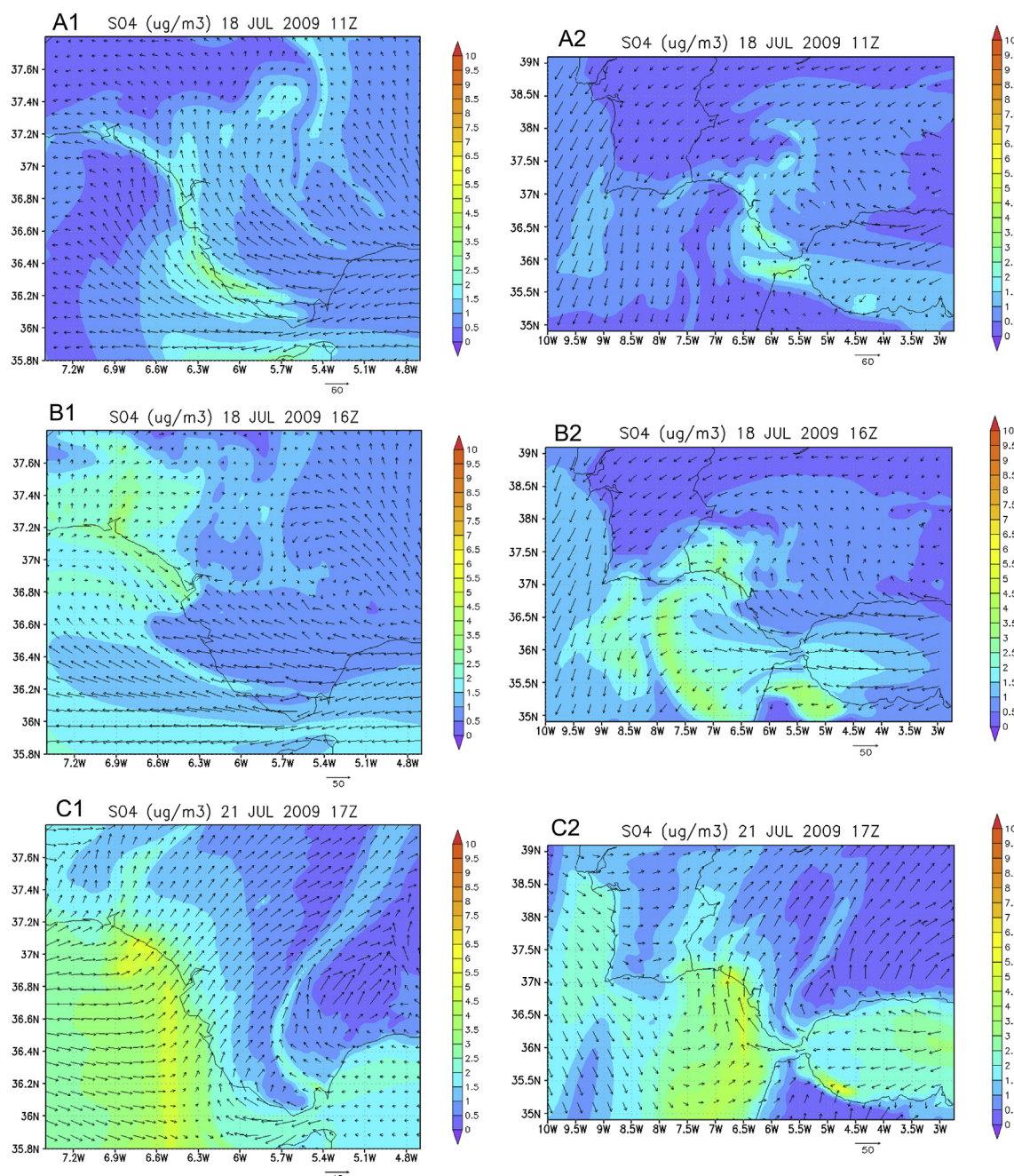


Fig. 13. a) Simulated and b) observed PM<sub>2.5</sub> sulphate (as ammonium sulphate) concentrations at Valverde, Univ. Campus and CIECEM sites. The arrows highlight example episodes showing influence of Algeciras (black arrow), Huelva (white arrow) and offshore emissions (grey arrow).



**Fig. 14.** Simulated surface  $PM_{2.5}$  sulphate concentration for A) 18/7/2009 11:00, B) 18/7/2009 16:00 and C) 21/7/2009 17:00 GMT for domain 3 ( $2\text{ km} \times 2\text{ km}$ ) (left panel) and domain 2 ( $6\text{ km} \times 6\text{ km}$ ) (right panel).

and Portugal interact. The situation is even more complex if other sources not included here, such as Moroccan and Algerian industrial emissions are also considered (e.g. Rodríguez et al., 2011).

#### 4. Conclusions

Detailed chemically speciated  $PM_{2.5}$  measurements obtained from four intensive field campaigns, simultaneously at three sites, are presented. In addition, a photochemical modelling system implemented with high temporal and spatial resolution ( $1\text{ h}$ ,  $2\text{ km} \times 2\text{ km}$ ) is presented and evaluated against this measurement database. The study area experiences a complex interaction of both high anthropogenic and biogenic emissions and exacerbating climate factors which contribute to high secondary aerosol

concentrations. Modelling performance varied according to component and season. The model captured the variability in the ammonium concentrations in both summer and winter periods, although it tended to underestimate the magnitude of concentrations, while for sulphate the performance was better during the summer periods. Some of the negative bias apparent in the  $PM_{2.5}$   $NH_4$  and  $SO_4$  simulated concentrations can likely be attributed to the lack of boundary conditions for aerosol species and this is identified as an area for future improvement of the modelling system.

The measured composition of  $PM_{2.5}$  showed that a significant fraction of sulphate (24–37%) and most of nitrate (79–94%) (averaged for all four campaigns) was not present as ammonium salts. Due to the correlation observed between non-ammonium nitrate and the excess of Na versus the Na/Cl ratio in sea salt, this was



attributed to the formation of  $\text{NaNO}_3$  by the heterogeneous reaction of nitric acid with sea salt. These features of nitrate predominantly as non-ammonium nitrate and a significant load of non-ammonium sulphate are considered typical features of southern Europe and are not typically observed in Central and Northern Europe. The formation of  $\text{NaNO}_3$  is often considered a coarse mode issue, due to  $\text{NaNO}_3$  being found dominantly in the coarse mode. However, although the dominant fraction (typically  $\sim 80\%$ ) of  $\text{NaNO}_3$  is found in the coarse mode (e.g. Alastuey et al., 2004) there is still a fraction of  $\text{NaNO}_3$  present in the fine mode. The results presented here show that, particularly in areas of southern Europe, the role of this fine mode  $\text{NaNO}_3$  is also extremely important and can dominate the  $\text{PM}_{2.5}$  nitrate composition. This has important implications for model simulations; it demonstrates that the chemical composition of particulate sulphate and particulate nitrate should be considered in both the measurement dataset and the model implementation when conducting the model evaluation. It also highlights the importance of including the formation of fine mode  $\text{NaNO}_3$  in model simulations which are often not included currently.

High temporal resolution measurements of BC were performed simultaneously at two sites providing the first such detailed measurements for this region and allowing an evaluation of the model PEC simulations at a fine time scale. The model  $\text{PM}_{2.5}$  PEC simulations performed well in capturing the diurnal variation in  $\text{PM}_{2.5}$  BC concentrations at the urban site as well as the substantial variability between seasons shown in the different campaigns, while underestimating the concentrations slightly. A larger underestimation of  $\text{PM}_{2.5}$  BC concentrations was observed at the rural site and this was attributed to the emission sources not being so well characterised for rural areas. Poorer model performance was observed for  $\text{PM}_{2.5}$  OC concentrations with a large underestimation observed during all campaigns.

An analysis of the model simulations evidences the complexity of the air management in the region, identifying scenarios of sulphate events linked to southern Spain emissions as well as to offshore shipping emissions and contributions from more distant emission sources such as Portugal.

This study has provided a detailed chemically speciated  $\text{PM}_{2.5}$  measurement database for a south-west region of Europe where the  $\text{PM}_{2.5}$  measurement composition is distinct from other areas of Europe. Such detailed measurements are often lacking when comparing observations against photochemical model simulations, and provide an opportunity not only to conduct a more robust and informative model evaluation but also to highlight areas of improvement for atmospheric aerosol modelling systems.

## Acknowledgements

The authors gratefully acknowledge funding from the Department of Innovation, Science and Enterprise of the Government of Andalusia through the research projects AER-REG (P07-RNM-03125) and SIMAND (P07-RNM-02729) and from the Department of Environment, Andalusian Regional Government (project: 199/2011/C/00). In addition, we thank the Spanish Ministry of Economy and Competitiveness for funding through the project POLLINDUST (CGL2011-26259). We would also like to thank the Government of Andalusia for providing data from their Air Quality Network and from their Atmospheric Emissions Inventory and AEMET for providing meteorological data.

## References

Aksoyoglu, S., Keller, J., Barmapadimos, I., Oderbolz, D., Lanz, V.A., Prévôt, A.S.H., Baltensperger, U., 2011. Aerosol modelling in Europe with a focus on

- Switzerland during summer and winter episodes. *Atmospheric Chemistry and Physics* 11, 7355–7373.
- Alastuey, A., Querol, X., Rodríguez, S., Plana, F., Lopez-Soler, A., Ruiz, C., Mantilla, E., 2004. Monitoring of atmospheric particulate matter around sources of secondary inorganic aerosol. *Atmospheric Environment* 38, 4979–4992.
- Athanasopoulou, E., Tombrou, M., Pandis, S.N., Russell, A.G., 2008. The role of sea-salt emissions and heterogeneous chemistry in the air quality of polluted coastal areas. *Atmospheric Chemistry and Physics* 8, 5755–5769.
- Baker, K., Scheff, P., 2007. Photochemical model performance for  $\text{PM}_{2.5}$  sulfate, nitrate, ammonium, and precursor species  $\text{SO}_2$ ,  $\text{HNO}_3$ , and  $\text{NH}_3$  at background monitor locations in the central and eastern United States. *Atmospheric Environment* 41, 6185–6195.
- Basart, S., Pay, M.T., Jorba, O., Pérez, C., Jiménez-Guerrero, P., Schulz, M., Baldasano, J.M., 2012. Aerosols in the CALIOPE air quality modelling system: evaluation and analysis of PM levels, optical depths and chemical composition over Europe. *Atmospheric Chemistry and Physics* 12, 3363–3392.
- Beekmann, M., Kerschbaumer, A., Reimer, E., Stern, R., Möller, D., 2007. PM measurement campaign HOVERT in the Greater Berlin area: model evaluation with chemically specified particulate matter observations for a one year period. *Atmospheric Chemistry and Physics* 7, 55–68.
- Boylan, J.W., Russell, A.G., 2006. PM and light extinction model performance metrics, goals, and criteria for three-dimensional air quality models. *Atmospheric Environment* 40, 4946–4959.
- Castell, N., 2008. Modelización aplicada a la evaluación y control de la contaminación fotoquímica en el Suroeste de la Península Ibérica. Ph.D. thesis. Universitat de València, p. 390 (in Spanish).
- Castell, N., Stein, A.F., Salvador, R., Mantilla, E., Millán, M., 2008. Sensitivity analysis of surface ozone to modified initial and boundary conditions in both rural and industrial zones. *Advances in Science and Research* 2, 113–118.
- Castell, N., Mantilla, E., Salvador, R., Stein, A.F., Millán, M., 2010a. Photochemical model evaluation of the surface ozone impact of a power plant in a heavily industrialized area of southwestern Spain. *Journal of Environmental Management* 91, 662–676.
- Castell, N., Stein, A.F., Mantilla, E., Salvador, R., Millán, M., 2010b. Evaluation of the use of photochemical indicators to assess ozone– $\text{NO}_x$ –VOC sensitivity in the Southwestern Iberian Peninsula. *Journal of Atmospheric Chemistry* 63, 73–91.
- Chang, J.S., Brost, R.A., Isaksen, I.S.A., Madronich, S., Middleton, P., Stockwell, W.R., Walcek, C.J., 1987. A three-dimensional Eulerian acid deposition model: physical concepts and formulation. *Journal of Geophysical Research* 92, 14,681–14,700.
- Chemel, C., Sokhi, R.S., Yu, Y., Hayman, G.D., Vincent, K.J., Dore, A.J., Tang, Y.S., Prain, H.D., Fisher, B.E.A., 2010. Evaluation of a CMAQ simulation at high resolution over the UK for the calendar year 2003. *Atmospheric Environment* 44, 2927–2939.
- COMAAN (Consejería de Medio Ambiente de Andalucía), 2006. Andalusian Atmospheric Emissions Inventory 2006. Andalusian Regional Government.
- de la Rosa, J.D., Sánchez de la Campa, A.M., Alastuey, A., Querol, X., González-Castanedo, Y., Fernández-Camacho, R., Stein, A.F., 2010. Using  $\text{PM}_{10}$  geochemical maps for defining the origin of atmospheric pollution in Andalusia (Southern Spain). *Atmospheric Environment* 44, 4595–4605.
- ENVIRON, 2008. Comprehensive Air Quality Model with Extensions (CAMx) Version 4.5. User's Guide. ENVIRON International Corporation.
- EPA, 2009. Speciation Profile Usage Memorandum. US Environmental Protection Agency. <http://www.epa.gov/ttn/chieff/index.html>.
- Fernández-Camacho, R., Rodríguez, S., de la Rosa, J., Sánchez de la Campa, A.M., Viana, M., Alastuey, A., Querol, X., 2010. Ultrafine particle formation in the inland sea breeze airflow in Southwest Europe. *Atmospheric Chemistry and Physics* 10, 9615–9630.
- Gaydos, T.M., Pinder, Rob, Koo, Bonyoung, Fahey, Kathleen M., Yarwood, Gregory, Pandis, Spyros N., 2007. Development and application of a three-dimensional aerosol chemical transport model, PMCAMx. *Atmospheric Environment* 41, 2594–2611.
- Grell, G.A., Dudhia, J., Stauffer, D.R., 1995. A Description of the Fifth-generation Penn State/NCAR Mesoscale Model (MM5). Tech. Rep. NCAR/TN-398+STR. National Center of Atmospheric Research (NCAR), USA.
- Guenther, A., Hewitt, C.N., Erickson, D., Fall, R., Geron, C., Graedel, T., Harley, P., Klinger, L., Lerdau, M., McKay, W.A., Pierce, T., Scholes, B., Steinbrecher, R., Tallamraju, R., Taylor, J., Zimmerman, P., 1995. A global model of natural volatile organic compound emissions. *Journal of Geophysical Research* 100, 8873–8892.
- Guenther, A., Zimmerman, P.R., Harley, P.C., Monson, R.K., Fall, R., 1993. Isoprene and monoterpenes emission rate variability: model evaluations and sensitivity analyses. *Journal of Geophysical Research* 98, 12609–12617.
- Harrison, R.M., Pio, C.A., 1983. Size differentiated composition of inorganic aerosol of both marine and polluted continental origin. *Atmospheric Environment* 17, 1733–1738.
- Intergovernmental Panel on Climate Change (IPCC), 2007. Fourth Assessment Report of the Intergovernmental Panel on Climate Change.
- Lazaridis, M., Spyridaki, A., Solberg, S., Smolik, J., Zdimal, V., Eleftheriadis, K., Aleksanropoulou, V., Hov, O., Georgopoulos, P.G., 2005. Mesoscale modeling of combined aerosol and photo-oxidant processes in the Eastern Mediterranean. *Atmospheric Chemistry and Physics* 5, 927–940.
- Li, G., Zavala, M., Lei, W., Tsimpidi, A.P., Karydis, V.A., Pandis, S.N., Canagaratna, M.R., Molina, L.T., 2011. Simulations of organic aerosol concentrations in Mexico City using the WRF-CHEM model during the MCMA-2006/MILAGRO campaign. *Atmospheric Chemistry and Physics* 11, 3789–3809.

- Lonati, G., Pirovano, G., Sghirlanzoni, G.A., Zanoni, A., 2010. Speciated fine particulate matter in Northern Italy: a whole year chemical and transport modelling reconstruction. *Atmospheric Research* 95, 496–514.
- Lopez, A.D., Mathers, C.D., Ezzati, M., Jamison, D.T., Murray, C.J.L., 2006. Global and regional burden of disease and risk factors, 2001: systematic analysis of population health data. *Lancet* 367, 1747–1757.
- Mathur, R., Yu, S., Kang, D., Schere, K.L., 2008. Assessment of the wintertime performance of developmental particulate matter forecasts with the Eta-Community Multiscale Air Quality modeling system. *Journal of Geophysical Research* 113, D02303. <http://dx.doi.org/10.1029/2007JD008580>.
- Moreno-Gutiérrez, J., Durán-Grados, V., Uriondo, Z., Ángel Llamas, J., 2012. Emission-factor uncertainties in maritime transport in the Strait of Gibraltar, Spain. *Atmospheric Measurement Techniques Discussions* 5, 5953–5991.
- Morris, R.E., Koo, B., Guenther, A., Yarwood, G., McNally, D., Tesche, T., Tonnesen, G., Boylan, J., Brewer, P., 2006. Model sensitivity evaluation for organic carbon using two multi-pollutant air quality models that simulate regional haze in the southeastern United States. *Atmospheric Environment* 40, 4960–4972.
- Nenes, A., Pilinis, C., Pandis, S.N., 1998. ISORROPIA: a new thermodynamic model for multiphase multicomponent inorganic aerosols. *Aquatic Geochemistry* 4, 123–152.
- Nenes, A., Pilinis, C., Pandis, S.N., 1999. Continued development and testing of a new thermodynamic aerosol module for urban and regional air quality models. *Atmospheric Environment* 33, 1553–1560.
- Pay, M.T., Jiménez-Guerrero, P., Jorba, O., Basart, S., Querol, X., Pandolfi, M., Baldasano, J.M., 2011. Spatio-temporal variability of concentrations and speciation of particulate matter across Spain in the CALIOPE modeling system. *Atmospheric Environment* 46, 376–396, 2012.
- Pey, J., Pérez, N., Querol, X., Alastuey, A., Cusack, M., Reche, C., 2010. Intense winter atmospheric pollution episodes affecting the Western Mediterranean. *Science of the Total Environment* 408, 1951–1959.
- Pope, C.A., Dockery, D.W., 2006. Health effects of fine particulate air pollution: lines that connect. *Journal of the Air and Waste Management Association* 56, 709–742.
- Pun, B.K., Balmori, R.T.F., Seigneur, C., 2009. Modeling wintertime particulate matter formation in central California. *Atmospheric Environment* 43, 402–409.
- Querol, X., Alastuey, A., Moreno, T., Viana, M.M., Castillo, S., Pey, J., Rodríguez, S., Artiñano, B., Salvador, P., Sánchez, M., García Dos Santos, S., Herce Garraleta, M.D., Fernandez-Patier, R., Mereno-Gau, S., Negral, L., Minguillón, M.C., Monfort, E., Sanz, M.J., Palomo-Marín, R., Pinilla-Gil, E., Cuevas, E., de la Rosa, J., Sánchez de la Campa, A., 2008. Spatial and temporal variations in airborne particulate matter (PM<sub>10</sub> and PM<sub>2.5</sub>) across Spain 1999–2005. *Atmospheric Environment* 42, 3964–3979.
- Querol, X., Alastuey, A., Rodríguez, S., Plana, F., Ruiz, C.R., Cots, N., Massagué, G., Puig, O., 2001. PM<sub>10</sub> and PM<sub>2.5</sub> source apportionment in the Barcelona Metropolitan area, Catalonia, Spain. *Atmospheric Environment* 35, 6407–6419.
- Renner, E., Wolke, R., 2010. Modelling the formation and atmospheric transport of secondary inorganic aerosols with special attention to regions with high ammonia emissions. *Atmospheric Environment* 44, 1904–1912.
- Rodríguez, S., Alastuey, A., Alonso-Pérez, S., Querol, X., Cuevas, E., Abreu-Afonso, J., Viana, M., Pérez, N., Pandolfi, M., de la Rosa, J., 2011. Transport of desert dust mixed with North African industrial pollutants in the subtropical Saharan Air Layer. *Atmospheric Chemistry and Physics* 11, 6663–6685.
- Rodríguez, S., Querol, X., Alastuey, A., de la Rosa, J., 2007a. Atmospheric particulate matter and air quality in the Mediterranean: a review. *Environmental Chemistry Letters* 5, 1–7.
- Rodríguez, S., Querol, X., Alastuey, A., Plana, F., 2002. Sources and processes affecting levels and composition of atmospheric aerosol in the Western Mediterranean. *Journal of Geophysical Research* 107 (D24), 4777.
- Rodríguez, S., Van Dingenen, R., Putaud, J.-P., Dell'Acqua, A., Pey, J., Querol, X., Alastuey, A., Chenery, S., Ho, K.-F., Harrison, R., Tardivo, R., Scarnato, B., Gemelli, V., 2007b. A study on the relationship between mass concentrations, chemistry and number size distribution of urban fine aerosols in Milan, Barcelona and London. *Atmospheric Chemistry and Physics* 7, 2217–2232.
- Sánchez de la Campa, A.M., de la Rosa, J., González-Castanedo, Y., Fernández-Camacho, R., Alastuey, A., Querol, X., Stein, A.F., Ramos, J.L., Rodríguez, S., Orellana, I.G., Nava, S., 2011. Levels and chemical composition of PM in a city near a large Cu-smelter in Spain. *Journal of Environmental Monitoring* 13, 1276.
- Sánchez de la Campa, A.M., de la Rosa, J., Querol, X., Alastuey, A., Mantilla, E., 2007. Geochemistry and origin of PM<sub>10</sub> in the Huelva region, Southwestern Spain. *Environmental Research* 103, 305–316.
- Schaap, M., Otjes, R.P., Weijers, E.P., 2011. Illustrating the benefit of using hourly monitoring data on secondary inorganic aerosol and its precursors for model evaluation. *Atmospheric Chemistry and Physics* 11, 11041–11053.
- Schlesinger, R.B., Kunzli, N., Hidy, G.M., Gotschi, T., Jerrett, M., 2006. The health relevance of ambient particulate matter characteristics: coherence of toxicological and epidemiological inferences. *Inhalation Toxicology* 18, 95–125.
- Simpson, D., Yttri, K.E., Klimont, Z., Kupiainen, K., Caseiro, A., Gelencsér, A., Pio, C., Puxbaum, H., Legrand, M., 2007. Modeling carbonaceous aerosol over Europe: analysis of the CARBOSOL and EMEP EC/OC campaigns. *Journal of Geophysical Research* 112, D23S14. <http://dx.doi.org/10.1029/2006JD008158>.
- Solazzo, E., Bianconi, R., Pirovano, G., et al., 2012. Operational model evaluation for particulate matter in Europe and North America in the context of AQMEII. *Atmospheric Environment* 53, 75–92.
- Strader, R., Lurmann, F., Pandis, S.N., 1999. Evaluation of secondary organic aerosol formation in winter. *Atmospheric Environment* 33, 4849–4863.
- Tesche, T.W., Morris, R., Tonnesen, G., McNally, D., Boylan, J., Brewer, P., 2006. CMAQ/CAMx annual 2002 performance evaluation over the eastern US. *Atmospheric Environment* 40, 4906–4919.
- Tsyro, S., Simpson, D., Tarrasón, L., Klimont, Z., Kupiainen, K., Pio, C., Yttri, K.E., 2007. Modeling of elemental carbon over Europe. *Journal of Geophysical Research* 112, D23S19. <http://dx.doi.org/10.1029/2006JD008164>.
- WHO, 2006. WHO Air Quality Guidelines for Particulate Matter, Ozone, Nitrogen Dioxide and Sulfur Dioxide: Global Update 2005. In: Summary of Risk Assessment. World Health Organization, Copenhagen.
- Yarwood, G., Rao, S., Yocke, M., Whitten, G.Z., 2005. Updates to the Carbon Bond Chemical Mechanism: CB05. Final Report to the U.S. EPA, RT-0400675.